Advanced Composite Materials
Publication details, including instructions for authors and subscription information:
http://www.tandfonline.com/loi/tacm20

Monitoring delamination of laminated CFRP using the electric potential change method (two-stage monitoring for robust estimation)

Masahito Ueda , Akira Todoroki , Yoshinobu Shimamura & Hideo Kobayashi

Version of record first published: 02 Apr 2012.

To cite this article: Masahito Ueda , Akira Todoroki , Yoshinobu Shimamura & Hideo Kobayashi (2005): Monitoring delamination of laminated CFRP using the electric potential change method (two-stage monitoring for robust estimation), Advanced Composite Materials, 14:1, 83-97

To link to this article: http://dx.doi.org/10.1163/1568551053297067

Adv. Composite Mater., Vol. 14, No. 1, pp. 83–97 (2005)

Monitoring delamination of laminated CFRP using the electric potential change method (two-stage monitoring for robust estimation)

MASAHITO UEDA *, AKIRA TODOROKI, YOSHINOBU SHIMAMURA and HIDEO KOBAYASHI

Department of Mechanical Sciences and Engineering, Tokyo Institute of Technology, 2-12-1, O-okayama, Meguro, Tokyo, 1528552, Japan

Received 7 July 2004; accepted 28 July 2004

Abstract—Detecting delaminations of carbon fiber reinforced plastic (CFRP) laminates is a difficult task for visual inspection. Delaminations cause large reductions in strength and stiffness of CFRP laminates, bringing deterioration of the structural reliability of a CFRP. Monitoring for delamination is, therefore, indispensable to maintain the reliability of a CFRP structure. In a previous study, we adopted the electric potential change method to detect delamination. This method shows good estimation performance for delamination cracks located near the edges of a specimen, but poor performance near the center where large errors that depend on the delamination shapes are created. A zigzag delamination caused by matrix cracking has a large effect on estimation performance; so the electric potential change method was not applicable to monitoring for delamination. In this paper, a mechanism that brings large errors of estimation due to the shape of the delamination is detailed. FEM analyses show a small electric current in the thickness direction in the center segment of a specimen causes large effects on the estimation performance. The problem is overcome by means of a newly proposed concept, a two-stage method. The effectiveness of the method is demonstrated using FEM analyses.

Keywords: Delamination; smart structure; health monitoring; response surface; inverse problem; electric potential; matrix crack.

1. INTRODUCTION

Carbon fiber reinforced plastic (CFRP) laminates are widely used in aerospace structures because of their superior mechanical properties. However, delamination can be easily induced in CFRP laminates by even a slight impact. Delamination causes large reductions in strength and stiffness of the CFRP laminate, bringing

*To whom correspondence should be addressed. E-mail: mueda@ginza.mes.titech.ac.jp

deterioration of the structural reliability of the CFRP. Therefore, monitoring for delamination is indispensable if the reliability of the CFRP structure is to be maintained.

Damage detection and strain measuring methods for a CFRP structure using its electrical conductivity have been proposed by many researchers [1–10]. Carbon fibers, which are electroconductive materials, make an electrical network by contacting each other; after delamination, the electrical network of carbon fibers is partially broken causing a change in the electric potential distribution. The delamination location and size are estimated by means of the electric potential change as an inverse problem. In this method, CFRP laminates are themselves used as a sensor. Electrodes are mounted on the surface to measure the electric potential at the electrodes. The applicability of this method has so far been shown only for conventional metallic materials [11–13].

This method has some advantages for a CFRP structure. First, because no sensor is embedded in the CFRP laminate it never reduces the strength or stiffness. Second, the method is easily applied at low cost just by mounting electrodes on the surface of a CFRP structure. This enables easy repairs when a system malfunctions. The authors have already employed an electric resistance change method (two-probe method) for identification of delamination; the applicability of the method was investigated analytically and experimentally using beam-type specimens and plate-type specimens [14–19].

Studies using the two-probe method have shown the effectiveness of the electric resistance change method for monitoring delamination of CFRP laminates by measuring the electric resistance change between adjacent electrodes. On the specimen surface, multiple electrodes were mounted by co-cured copper foil to measure the electric resistance changes. A response surface was employed as a solver of the inverse problem instead of an artificial neural network. The method successfully identified the location and size of a delamination. The data-normalization method provided significant improvement of estimation performance [18].

The method, however, requires a lot of switching circuits to apply an electric current between all adjacent electrodes and the estimation accuracy is strongly affected by the condition of the electric contact between the copper electrodes and the carbon fibers. To overcome these problems, the electric potential change method was introduced in our earlier study. This method measures the electric potentials by the charging electric current at the two electrodes, which are made at the opposite ends of a beam type specimen. Our earlier study showed that this electric potential change method provides poor estimation performance analytically [20, 21] and experimentally [22] when compared with the results of the electric resistance change method. However, the data-normalization method remarkably improved the performance of estimations of straight delaminations [23].

It is expensive obtaining all the data from experiments making response surfaces; hence FEM analyses should be conducted instead of the experiments. Although the actual delamination cracks generally present zigzag shapes due to matrix cracking, it is impossible to make a response surface after considering all the shapes of the delaminations even for FEM analyses. Therefore, if the electric potential changes could be calculated using the FEM analyses without considering the zigzag cracks, it would greatly help to reduce the computational costs. That is, practical cracks with zigzag shapes can be estimated using the response surfaces made from the FEM analyses of straight delaminations. In an earlier study of ours, the difference of the electric resistance change between a straight delamination and a zigzag shape crack was demonstrated for the electric resistance change method (two-probe method) [19]; clarifying that the difference is small and that the difference did not affect the estimation performance for the electric resistance change method. However, for the electric potential change method, when a delamination crack is located at the center segment of the charged electrodes, the shapes of the delamination crack strongly affect the estimation performance. Large errors were obtained at the segment when zigzag shape cracks such as a Z-type or an inverse Z-type delamination crack were estimated using the response surfaces made from analyses of straight delaminations [23].

In this paper, a mechanism that creates large estimation errors due to the delamination shape is detailed. From the point of view of practical application, zigzag shape cracks need to be estimated using the response surface made from FEM analyses of straight delaminations. In other words, the response surface should be robust against various shapes of delamination cracks. The problem is overcome by means of a new concept, the two-stage estimation method; its effectiveness is shown by FEM analyses.

2. ANALYTICAL METHOD AND RESULT OF ESTIMATION

2.1. Analytical model

In this study, FEM analyses are performed with the commercially available FEM code ANSYS. The specimen is a two-dimensional beam with a configuration of 200 mm length and 1 mm thickness, as shown in Fig. 1. The stacking sequence of the specimen is [0/90]s , and the thickness of a ply is approximately 0.25 mm.

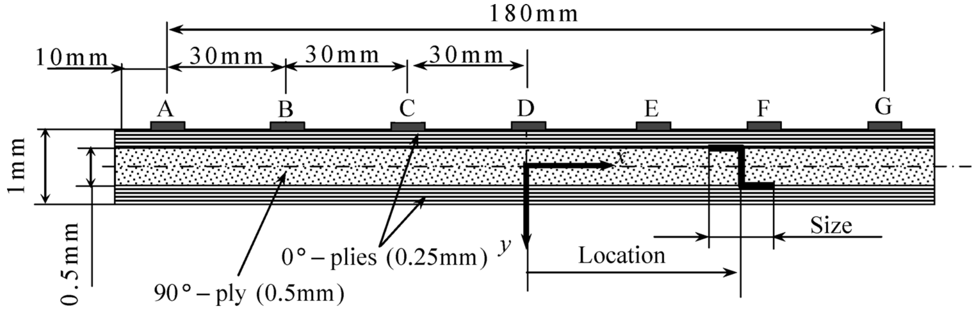

Figure 1. Analytical model of laminated CFRP.

Table 1.
Conductivity ratio of CFRP ($V_f = 0.472$)

V_f (vol%)	σ_{90}/σ_0	σ_t/σ_0	σ_0 ($m^{-1}\ \Omega^{-1}$)
0.472	1.05×10^{-3}	2.24×10^{-4}	4.6×10^3

Seven electrodes, each 5 mm in width, are mounted on one surface of the specimen at spacings of 30 mm. It is assumed that the electrodes are mounted only on the inside surface of shell-type CFRP structures. The electric potential of the FEM grids at the electrodes are coupled to have the same electric potential with each other.

For the cross-ply composites, the electric current flows not only in the longitudinal direction, but also in the thickness direction of the specimen. Since the electric current is impeded by the presence of a delamination, the delamination can be detected by means of measuring the electric potential change between the electrodes.

Quadratic four-node elements 0.0625 mm in height and 0.25 mm in length are used for the FEM calculations. Electric conductivity used in the FEM analyses is shown in Table 1. This electric conductivity is obtained from the experimental results of a CFRP laminate having a fiber volume fraction $V_f = 0.472$. σ_0, σ_{90} and σ_t are the conductivities of the longitudinal, transverse and thickness directions, respectively. The conductivity in the thickness direction includes the effect of resin rich layers between plies.

2.2. Solver of inverse problem

Response surface methodology is applied to identify a delamination in a CFRP laminate. Details of the response surface methodology are shown in Ref. [24]. The following quadratic polynomial is adopted as a response surface:

$$y = \beta_0 + \sum_{i=1}^{n} \beta_i x_i + \sum_{i=1}^{n} \beta_{ii} x_i^2 + \sum_{j=1}^{n-1} \sum_{i=j+1}^{n} \beta_{ji} x_j x_i. \qquad (1)$$

Our earlier studies demonstrated that the quadratic polynomial possessed high estimation performance for this inverse problem [14–19]. An electric current of 50 mA is applied at the end-electrode A of a beam type specimen and the other end-electrode G is set to be 0 V. The electric potentials at the electrodes are measured before and after creating a delamination. The electric potential differences P_i ($i = 1$ to 6) between the electrodes AD, BD, CD, DE, DF, DG are calculated. FEM analyses are conducted for the multiple cases: delamination sizes of 5, 7, 10, 15, 20, 25, 30, 35 and 40 mm: delamination locations from −90 mm to 90 mm with spacing of 5 mm. FEM runs of 315 are performed.

The electric potential change ratios $\Delta P_i / P_{i0}$ are calculated from the electric potential differences between the electrodes. These electric potential change ratios are normalized by the norm of the electric potential change vector [18]. The normalization transforms the electric potential change ratios of all electric potential differences to a unit vector by dividing those by the norm. The predictor variables of the response surfaces are normalized electric potential change ratios and norms. The response variables are delamination location and size.

$$\frac{\Delta p_i}{p_{i0}} = \frac{\Delta P_i / P_{i0}}{L} \quad (i = 1 \sim 6),$$
$$L = \sqrt{\sum_{k=0}^{6} (\Delta P_k / P_{k0})^2}. \tag{2}$$

When a regression coefficient has a low contribution to the regression, the coefficient is eliminated from the response surface to maximize the adjusted coefficient of multiple determination R^2_{adj}.

2.3. Shapes of delamination

Three delamination shapes are investigated in this paper: straight, Z-type and inverse Z-type delamination cracks (Fig. 2). The straight delamination is placed at the interlamina near the electrodes because a large delamination is generally created at the opposite interlamina to the impacted surface (the impacted surface is the opposite surface to the surface on which all electrodes are mounted). A Z-type delamination crack has two same-length delaminations, one at each end of the matrix crack as shown in Fig. 2. The inverse Z-type delamination crack is a symmetrical shape of the Z-type delamination crack. The delamination length of the upper and lower ends of the matrix crack is assumed to be the same length in this paper because the largest differences are expected in them compared with the straight delamination, as shown in an earlier study [19].

The coordinates are defined as shown in Fig. 1. The definition of the delamination location is the distance from the origin to the center of the delamination or the location of the matrix crack. The definition of the delamination size is a length

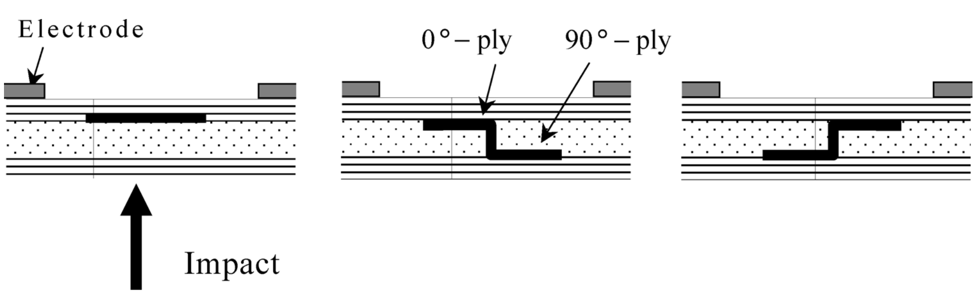

Figure 2. Types of delamination crack shape. (a) Straight delamination (without matrix crack). (b) Z-type delamination crack (with matrix crack). (c) Inverse Z-type delamination crack (with matrix crack).

projected onto the specimen surface. In the FEM analysis, delamination is created by means of separating two nodes that are placed at same position. It is assumed in the FEM analyses that the electric current does not flow through the delamination.

As previously described, Z-type and inverse Z-type delamination cracks are analyzed to investigate the effect of the delamination shape on the estimation performance: for the estimation, response surfaces are made from FEM analyses of straight delaminations. This is to check the robustness of response surfaces against various shapes of delaminations.

2.4. Results of the estimations

In our earlier study, two response surfaces for estimation of the delamination locations and sizes were made from FEM analyses of straight delaminations by charging electric currents at the end-electrodes of a beam type specimen [23]. The adjusted coefficients of multiple determinations R^2_{adj} are 0.9988 for the delamination location and 0.9251 for the delamination size. When the adjusted coefficients of multiple determinations R^2_{adj} are close to 1, good regressions are indicated. The electric potential change method showed good estimation performance of straight delaminations by applying data-normalization. The estimations of Z-type or inverse Z-type delamination cracks, however, were poor when the cracks were located at the center segment of the charged electrodes. Large estimation errors of the size were created when the delamination size was 15 mm or smaller. For example, a zigzag crack of 7 mm was estimated as −40 mm. For the estimation of the location of the delamination, poor estimation results were also observed at the center segment of the specimen, although the other estimations were excellent. The shapes of the delamination did not affect the estimation performance when using the electric resistance change method [19]. However, the electric potential change method was strongly affected by the delamination shape when the location of the delamination crack was at the center segment of the specimen.

3. MECHANISM OF THE DIFFERENT ELECTRIC POTENTIAL CHANGE DUE TO THE DELAMINATION SHAPE

Figure 3 shows a contour plot of the electric potential inside a specimen when an electric current is charged at end-electrode A and the other end-electrode G is set to be 0 V. The abscissa and the ordinate show the longitudinal and the thickness directions of the specimen respectively. The electric current flows in the thickness direction under the charged electrodes A and G. This indicates that the electric current flows not only in the upper 0°-ply but also in the lower 0°-ply. However, at the center segment of the specimen the contour plot is perpendicular to the specimen surface. This means that the electric current flows only in the longitudinal direction. Figure 4 shows the electric current density in the longitudinal direction at the center of the specimen ($x = 0$ mm). The abscissa shows the electric current density in

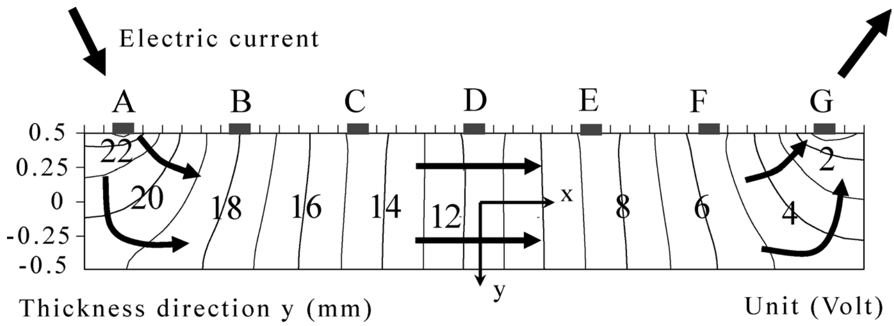

Figure 3. Contour plot of electric potential in cross-ply CFRP beam.

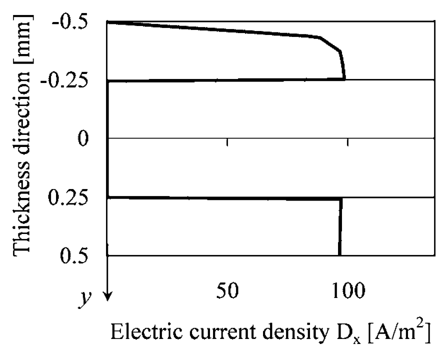

Figure 4. Electric current density in the longitudinal direction at $x = 0$ mm.

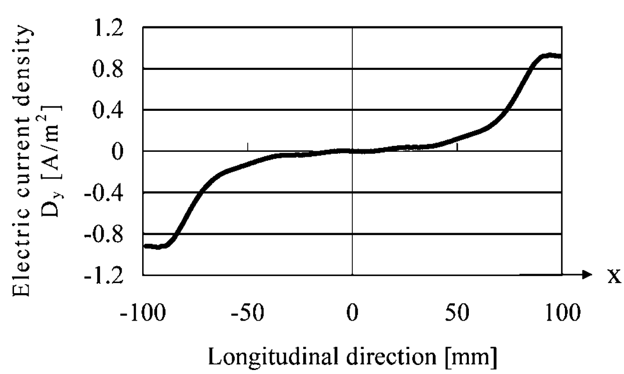

Figure 5. Electric current density in the thickness direction at $y = -0.25$ mm.

the longitudinal direction and the ordinate shows the thickness direction of the specimen. Almost half of the electric current flows in the lower 0°-ply. Figure 5 shows the electric current density in the thickness direction at the interlamina between the surface 0°-ply and the 90°-ply near the electrode ($y = -0.25$ mm). The abscissa and the ordinate show the longitudinal direction and the electric current density in the thickness direction, respectively. No electric current flows in the thickness direction at the center of the specimen.

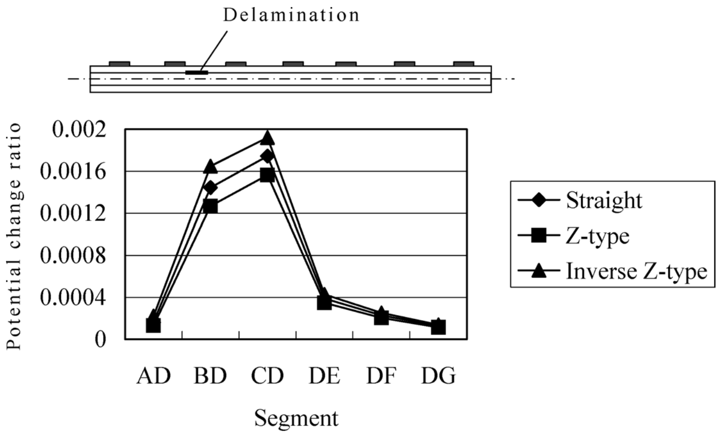

(a)

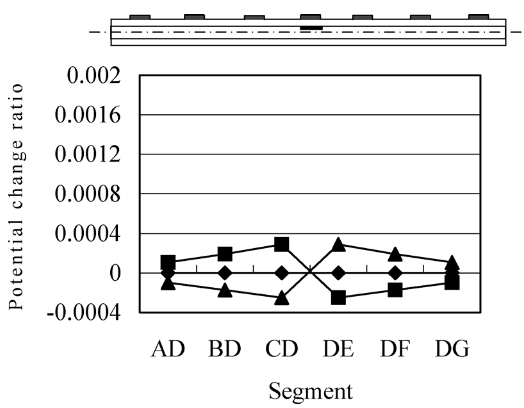

(b)

Figure 6. Electric potential change ratios without normalization (delamination size is 5 mm). (a) Delamination locates at $x = -50$ mm (delamination size is 5 mm). (b) Delamination locates at $x = 0$ mm (delamination size is 5 mm).

Figure 6a and b, shows the electric potential change ratios before normalization in the case of a 5 mm delamination and delamination locations of −50 mm and 0 mm. The electric potential change ratios are almost the same as each other, and the results do not depend on the delamination shapes when delaminations are located near the charged electrode A (Fig. 6a). This is because much of the electric current is impeded by the delamination at the interlamina and a little electric current is impeded by the matrix cracking in the middle 90°-ply. However, the electric potential change ratios are quite small when the delaminations are located at the center of the specimen because most of the electric current flows in the longitudinal direction in both 0°-plies (Fig. 6b). A difference due to the delamination shapes is recognized because of the low electric current in the thickness direction. Figure 7 shows the electric potential change ratios after data-normalization in this case.

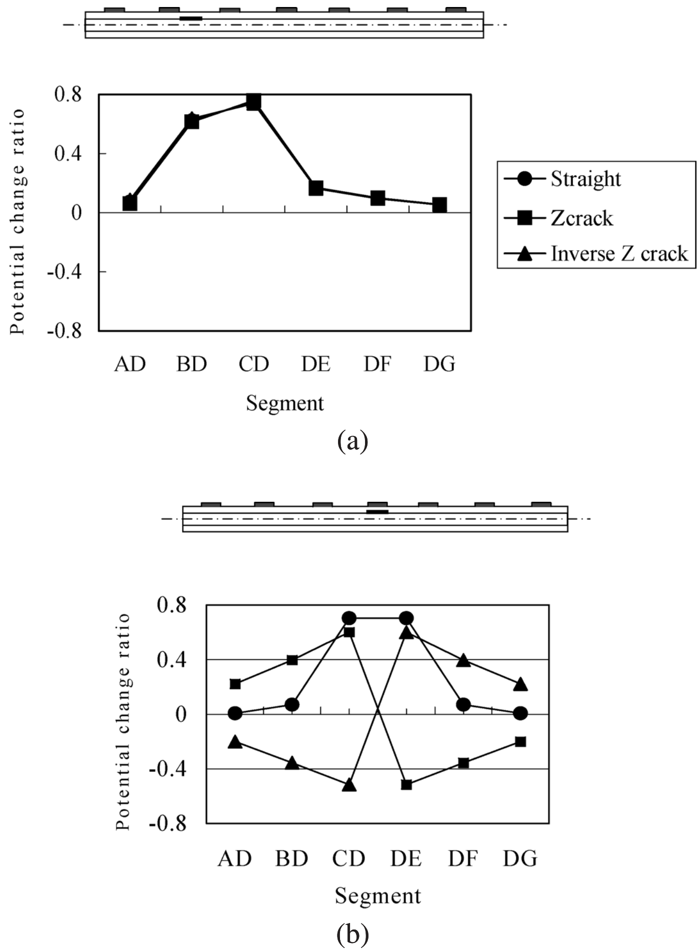

Figure 7. Normalized electric potential change ratios (delamination size is 5 mm). (a) Delamination locates at $x = -50$ mm (delamination size is 5 mm). (b) Delamination locates at $x = 0$ mm (delamination size is 5 mm).

The data-normalization method magnifies those small differences of the electric potential change ratios caused by the delamination shapes.

Data-normalization was successfully applied to the electric resistance change method (two-probe method); in which sufficient electric current flows in the thickness direction compared with the flows in the longitudinal direction in the middle 90°-ply layer. The larger electric flow makes a large electric resistance change without any relationship with the matrix crack in the middle 90°-ply layer (delamination shapes), whereas, with the electric potential change method, the electric current is charged at the end-electrodes of the specimen. The electric current in the thickness direction is very low around the center of the specimen because of the long spacing between charged electrodes. As a result, the electric potential change ratios are strongly affected by the matrix crack in the middle 90°-ply layer (delamination shapes) although the values themselves are very small. The small values are magnified by the data-normalization; which causes large errors when Z-type or inverse Z-type delamination cracks are estimated using response surfaces made from analyses of straight delaminations.

4. TWO-STAGE ESTIMATION METHOD

The electric potential change ratios are small when delamination cracks are located at the center segment of the specimen because of the low electric current in the thickness direction. The small differences due to the delamination shapes are magnified by data-normalization; thus, poor estimations are created at the center segment of the specimen. Zigzag cracks, however, can be estimated with excellent performance outside the electrodes CE. Delamination cracks, therefore, can be classified into two areas by estimations of their location; into the center segment between the electrodes CE or outside this segment [23]. After estimation of location, an extra estimation is conducted as a second stage to estimate a delamination in the segment inside the electrodes CE.

The second-stage estimation is as follows. The electric current is charged from the center electrode D to both end-electrodes A and G to increase the electric current in the thickness direction at the center segment. By charging the electric current at the center electrode, the estimation performance at the center segment is improved, causing a more robust estimation against the delamination shape because of the high electric current in the thickness direction (Fig. 8).

An electric current of 50 mA is charged at the center-electrode D of a beam type specimen, and the two end-electrodes A and G are set to be 0 V. Electric potentials at the electrodes are then measured before and after the creation of a delamination. The electric potential differences P_i ($i = 1$ to 5) between electrodes AB, AC, AD, EG, FG are calculated. FEM analyses are conducted for the multiple cases: delamination sizes of 5, 7, 10, 15, 20, 25, 30, 35 and 40 mm: delamination locations

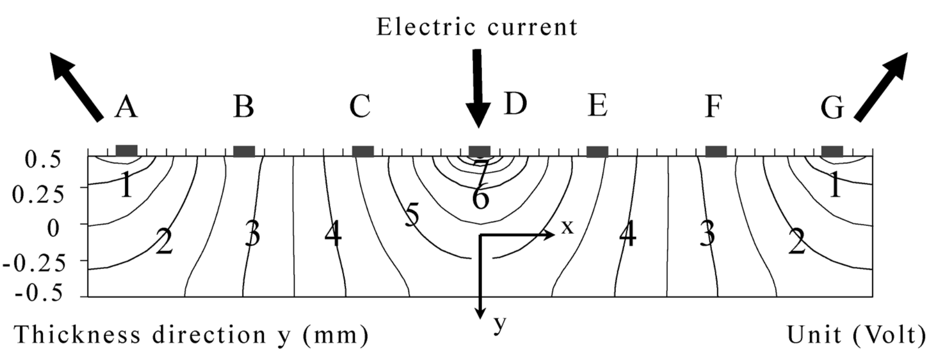

Figure 8. Contour plot of electric potential in CFRP beam when electric current is charged at the center electrode D.

from −30 mm (at electrode C) to 30 mm (at electrode E) with spacings of 5 mm. FEM runs of 117 are performed.

The response surfaces for the delamination location and size are made from analyses of straight delaminations. Figures 9 and 10 are the estimation results of location and size of a straight delamination. The abscissa shows either delamination location or size and the ordinate shows estimated location or size. The diagonal lines in the figures indicate an exact estimation. The broken lines in the figures show the error band of ±5 mm. Response surfaces are made using the linear model because (1) the linear model possess good enough performance of estimation in this case and (2) the model is robust against the experimental error: the higher order model is

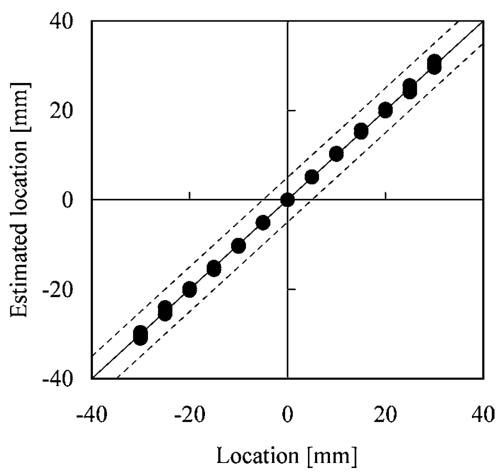

Figure 9. Estimated location of straight delamination between electrodes CE using the response surface made from analyses of straight delaminations ($R^2_{adj} = 0.9996$).

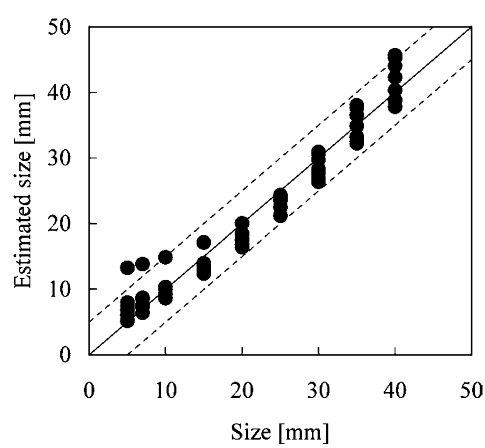

Figure 10. Estimated size of straight delamination between electrodes CE using the response surface made from analyses of straight delaminations ($R^2_{adj} = 0.9472$).

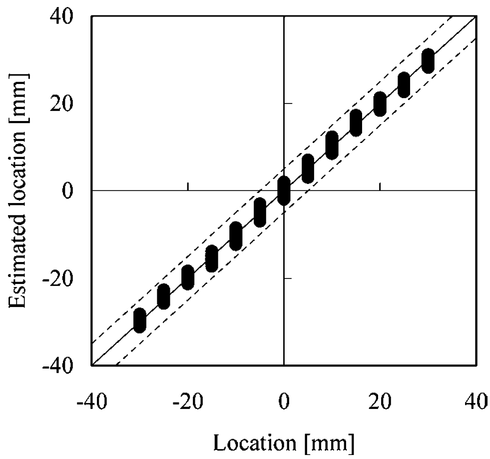

Figure 11. Estimated location of Z-type and inverse Z-type delamination cracks between electrodes CE using the response surface made from analyses of straight delaminations.

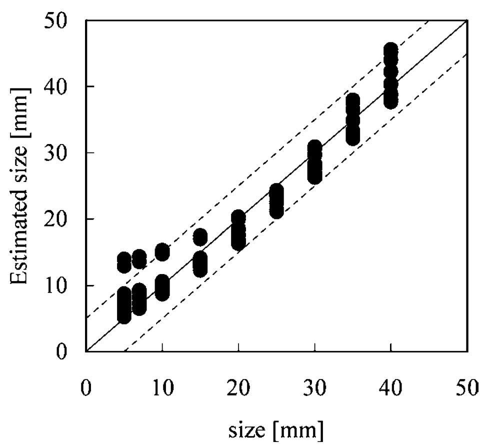

Figure 12. Estimated size of Z-type and inverse Z-type delamination cracks between electrodes CE using the response surface made from analyses of straight delaminations.

often sensitive to the errors. The adjusted coefficients of multiple determinations are 0.9996 for delamination location and 0.9472 for delamination size with the linear model.

Figures 11 and 12 show the estimation results of location and size of Z-type and inverse Z-type delamination cracks using the response surfaces made from analyses of straight delaminations. The abscissa and the ordinate are the same with Figs 9 and 10. The Z-type and inverse Z-type delamination cracks can be estimated with excellent performance although they are located at the center segment of the specimen.

The electric potential change ratios after data-normalization are shown in Fig. 13. The delamination location is the center of the specimen and delamination size

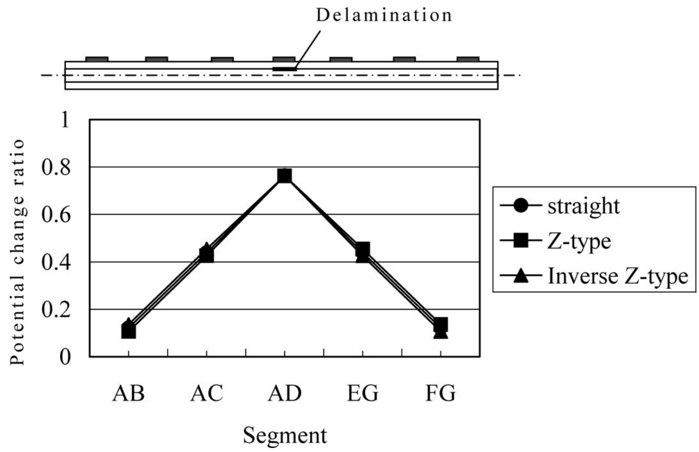

Figure 13. Normalized electric potential change ratios between the electrodes when an electric current is charged at electrode D (delamination location is $x = 0$ mm and delamination size is 5 mm).

is 5 mm. The abscissa shows the electrodes at which the electric potentials are measured, and the ordinate shows the normalized electric potential change ratios. Differences due to the delamination shapes are quite small, although the delamination cracks are located at the center of the specimen. The electric potential change due to delamination at the interlamina as an impediment of electric current in the thickness direction is increased by the high electric current in the thickness direction.

5. CONCLUSIONS

Delamination cracks in a cross-ply laminate were estimated using the electric potential change method. The estimation performance dropped when a zigzag crack was located at the center segment of the specimen. To overcome the problem, a new two-stage estimation method has been introduced. The results obtained in this paper can be summarized as follows.

(i) With the electric potential change method, the density of the electric current in the thickness direction decreases at the center segment of the specimen. Since the electric potential change is small at the segment because of the low electric current in the thickness direction, the small difference in the electric potential changes due to the delamination shapes remains. These small electric potential change ratios that depend on the delamination shapes are magnified by data-normalization. Zigzag shaped delamination cracks, therefore, could not be estimated using the response surface made from FEM analyses of straight delaminations.

(ii) The decrease of the electric current in the thickness direction caused large estimation errors. To overcome the problem, an electric current is charged at the center electrode when the delamination crack is located at the center segment of the specimen. Delamination cracks are classified by the ordinary electric potential change method into two areas: center or the outer segments of the specimen. Electric current is charged at the center-electrode when a delamination crack is estimated to be in the center segment.

(iii) A delamination that is located in the outer segments of a specimen is estimated with excellent performance regardless of the delamination shape. When a delamination is estimated to be in the center segment of the specimen by a first-stage estimation, the delamination is estimated by charging an electric current at the center electrode in a second-stage estimation. FEM analyses demonstrate that the effectiveness of the two-stage estimation method is excellent.

REFERENCES

1. K. Moriya and T. Endo, A study on flaw detection method for CFRP composite laminates (1st report), *J. Jpn. Soc. for Aeronautical and Space Sci.* **36** (410), 139–146 (1988).
2. K. Schulte and C. Baron, Load and failure analyses of CFRP laminates by means of electrical resistivity measurements, *Compos. Sci. Technol.* **36** (1), 63–76 (1989).
3. P. W. Chen and D. D. L. Chung, Carbon fiber reinforced concrete for smart structures capable of non-destructive flaw detection, *Smart Mater. Struct.* **2** (1), 22–30 (1993).
4. P. E. Irving and C. Thiagarajan, Fatigue damage characterization in carbon fibre composite materials using an electrical potential technique, *Smart Mater. Struct.* **7** (4), 456–466 (1998).
5. J. C. Abry, S. Bochard, A. Chateauminois, M. Salvia and G. Giraud, In situ detection of damage in CFRP laminates by electrical resistance measurements, *Compos. Sci. Technol.* **59** (6), 925–935 (1999).
6. D. C. Seo and J. J. Lee, Damage detection of CFRP laminates using electrical resistance measurement and neural network, *Composite Structures* **47** (1-4), 525–530 (1999).
7. I. Weber and P. Schwartz, Monitoring bending fatigue in carbon-fibre/epoxy composite strands: a comparison between mechanical and resistance techniques, *Compos. Sci. Technol.* **61** (6), 849–853 (2001).
8. N. Muto, Y. Arai, S. G. Shin, H. Matsubara, H. Yanagida, M. Sugita and T. Nakatsuji, Hybrid composites with self-diagnosing function for preventing fatal fracture, *Compos. Sci. Technol.* **61** (6), 875–883 (2001).
9. S. Kubo, M. Kuchinishi, T. Sakagami and S. Ioka, Identification of delamination in layered composite materials by the electric potential CT method, *Int. J. Jpn. Soc. Appl. Electromagn. Mech.* **15** (1/4), 261–267 (2001).
10. J. B. Park, T. Okabe, N. Takeda and W. A. Curtin, Electromechanical modeling of unidirectional CFRP composites under tensile loading condition, *Composites: Part A* **33** (2), 267–275 (2002).
11. C. N. Owston, Eddy current methods for the examination of carbon fibre reinforced epoxy resins, *Mater. Eval.* **34** (11), 237–244 (1976).
12. T. Sakagami, S. Kubo and K. Ohji, Crack identification by the electric potential CT inverse analyses incorporating optimization techniques, *Engineering Analysis with Boundary Elements* **7** (2), 59–65 (1990).
13. N. Tada, Y. Hayashi, T. Kitamura and R. Ohtani, Analysis on the applicability of direct current electrical potential method to the detection of damage by multiple small internal cracks, *Int. J. Fract.* **85** (1), 1–9 (1997).

14. A. Todoroki, The effect of number of electrodes and diagnostic tool for monitoring the delamination of CFRP laminates by changes in electrical resistance, *Compos. Sci. Technol.* **61** (13), 1871–1880 (2001).
15. A. Todoroki and Y. Tanaka, Delamination identification of cross-ply graphite/epoxy composite beams using electric resistance change method, *Compos. Sci. Technol*. **62** (5), 629–639 (2002).
16. A. Todoroki, Y. Tanaka and Y. Shimamura, Delamination monitoring of graphite/epoxy laminated composite plate of electric resistance change method, *Compos. Sci. Technol.* **62** (9), 1151–1160 (2002).
17. A. Todoroki, M. Tanaka and Y. Shimamura, Measurement of orthotropic electric conductance of CFRP laminates and analysis of the effect on delamination monitoring with an electric resistance change method, *Compos. Sci. Technol.* **62** (5), 619–628 (2002).
18. A. Todoroki, M. Tanaka and Y. Shimamura, High performance estimations of delamination of graphite/epoxy laminates with electric resistance change method, *Compos. Sci. Technol.* **63** (13), 1911–1920 (2003).
19. A. Todoroki, M. Tanaka, Y. Shimamura and H. Kobayashi, Analysis of the effect of the configuration of the delamination crack on delamination monitoring with electric resistance change method, *J. Jpn. Soc. Compos. Mater.* **29** (3), 113–119 (2003).
20. A. Todoroki, H. Suzuki and Y. Shimamura, Identification of delamination cracks of CFRP by electrical potential method, *J. Jpn. Soc. Mech. Engng (A)* **65** (634), 1330–1336 (1999).
21. A. Todoroki and H. Suzuki, Health monitoring of internal delamination cracks for graphite/epoxy composites by electric potential method, *Appl. Mech. Engng* **5** (1), 283–294 (2000).
22. A. Todoroki, Y. Tanaka, Y. Shimamura and H. Kobayashi, Smart structure for detection of embedded delamination of CFRP plates using multi-point voltage change, *J. Jpn. Soc. Mech. Engng (A)* **67** (658), 1002–1008 (2001).
23. M. Ueda, A. Todoroki, Y. Shimamura and H. Kobayashi, Monitoring delamination of laminated CFRP using the electric potential change method: Application of normalization method and the effect of the shape of a delamination crack, *Adv. Composite Mater.* **13**, 311–324 (2004).
24. R. H. Myers and D. C. Montgomery, *Response Surface Methodology: Process and Product Optimization Using Designed Experiments*, 2nd edn. John Wiley, New York (2002).